

STUDIES OF SYSTEMATIC UNCERTAINTIES OF POLARIZATION ESTIMATION FOR EXPERIMENTS WITH THE WASA DETECTOR AT COSY*

M. HODANA, P. MOSKAL, I. OZERIANSKA

The Marian Smoluchowski Institute of Physics, Jagiellonian University
Reymonta 4, Kraków, Poland
and

Experimental Hadron Structure (IKP-1), Forschungszentrum Jülich
Wilhelm-Johnen-Straße 52428 Jülich, Germany

(Received August 23, 2013)

In November 2010, the azimuthally symmetric WASA detector and the polarized proton beam of COSY have been used to collect a high statistics sample of $\vec{p}p \rightarrow pp\eta$ reactions in order to determine the analyzing power as a function of the invariant mass spectra of the two-particle subsystems. Here, we show studies of the influence of the beam and target characteristics such as location and direction on the determination of degree of the polarization.

DOI:10.5506/APhysPolBSupp.6.1041

PACS numbers: 13.88.+e, 24.70.+s

1. Introduction

In the last decade, a vast set of unpolarized cross sections has been determined for the η production in the collision of nucleons [1–12]. However, the understanding of the production mechanism of this meson still requires determination of spin observables. Up to now, there are only three measurements of the analyzing power for the $\vec{p}p \rightarrow pp\eta$ reaction which have been performed with low statistics and the determined value of analyzing power is essentially consistent with zero [13–15] within large error bars of about ± 0.15 . The WASA detector installed at the Cooler Synchrotron COSY gives a possibility to measure the analyzing power with high statistics and high acceptance. Therefore, in November 2010, we have conducted an exclusive measurement of the $\vec{p}p \rightarrow pp\eta$ reaction using the polarized proton beam of

* Presented at the Symposium on Applied Nuclear Physics and Innovative Technologies, Kraków, Poland, June 3–6, 2013.

the COSY synchrotron and the WASA detector [16]. The measurement was performed for two beam momenta corresponding to 15 MeV and 72 MeV excess energies. The choice of these values of excess energies was dictated by the availability of the data for the spin averaged cross sections obtained previously at COSY-11 [2], TOF [1] and WASA/CELSIUS [3] experiments.

For the purpose of the monitoring of the degree of polarization, concurrently to the $\vec{p}p \rightarrow pp\eta$ reaction, a proton-proton elastic scattering reactions have been measured. In this contribution, we present an estimation of systematic uncertainties of the determination of the degree of polarization of the COSY beam based on the elastically scattered protons measured by means of the WASA detector setup.

2. Polarization

The polarization is extracted using the following formula

$$P(\theta) = \frac{1}{A_y(\theta) \cos \phi} \frac{N(\theta, \phi) - N(\theta, \phi + \pi)}{N(\theta, \phi) + N(\theta, \phi + \pi)}, \quad (1)$$

where θ is the scattering angle of the forward going proton calculated in the centre-of-mass frame, ϕ is its azimuthal angle, N denotes the number of events and $A_y(\theta)$ is the analyzing power of the $\vec{p}p \rightarrow pp$ reaction which was extracted from the results of the EDDA Collaboration [17].

The asymmetry, $\epsilon(\theta, \phi)$, is defined as

$$\epsilon(\theta, \phi) = \frac{N(\theta, \phi) - N(\theta, \phi + \pi)}{N(\theta, \phi) + N(\theta, \phi + \pi)} \quad (2)$$

and, according to Eq. (1), it can be written as

$$\epsilon(\theta, \phi) = p_0 \cos(\phi), \quad (3)$$

where $p_0 = P(\theta) A_y(\theta)$. Polarization is, therefore, extracted by fitting of function given by Eq. (3) to a $\epsilon(\theta, \phi)$ distributions as shown in Fig. 1.

Asymmetry is calculated separately for each spin orientation of polarized protons, in four ranges of protons' scattering angle starting from 30° up to 46° in steps of 4°. As a result, four polarizations are extracted for four ranges of the center-of-mass polar angle of the forward scattered proton, θ_{CMs} . The final polarization for a given spin is then calculated as a weighted mean

$$P = \frac{\sum_{i=1}^n P(\theta_i) / \sigma_{P(\theta_i)}^2}{\sum_{i=1}^n 1 / \sigma_{P(\theta_i)}^2}, \quad (4)$$

where θ_i is the scattering angle of the forward going proton, calculated in the centre-of-mass system.

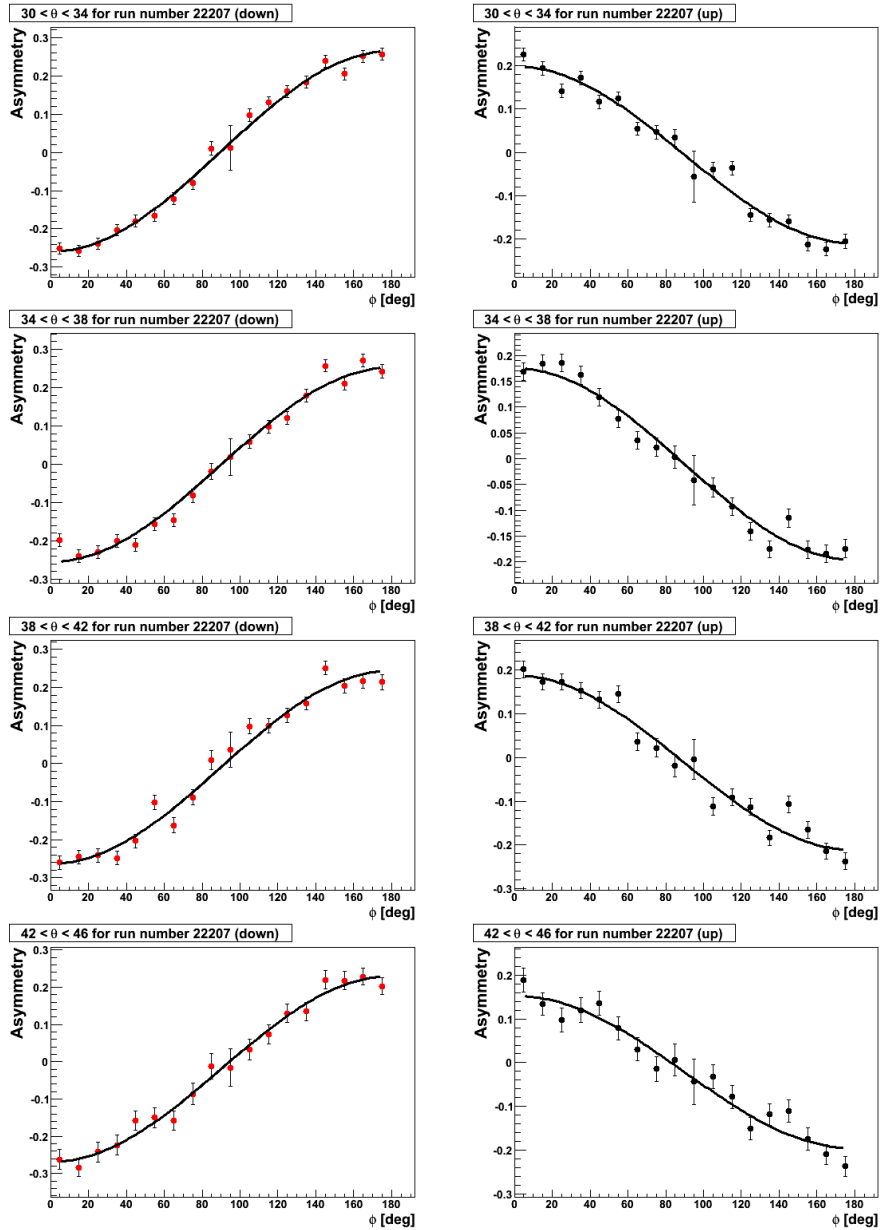


Fig. 1. Experimental distributions of the asymmetry as a function of the proton's azimuthal angle, made for the proton's scattered into an angle given in histograms' title boxes. Black line represents the fit function given by Eq. (3). Left panel: protons with spin down. Right panel: protons with spin up.

2.1. Position of the vertex

The probable source of the systematic uncertainty in the determination of the polarization might be false number of events in the individual θ_{CMs} ranges, originating from the possible misalignment of the beam's and/or target's position.

The reconstruction of tracks of particles registered in the Mini Drift Chamber is free of any assumption of the position of the reaction vertex. In this respect, obtained angular information can be assumed to reflect actual situation of particles going through the Mini Drift Chamber. Reconstruction of tracks of particles going in the forward direction, however, is based on the assumption that the interaction point is located at $(x_v, y_v, z_v) = (0, 0, 0)$. This may contribute to the systematic uncertainty of the polarization. To determine the size of this contribution, studies on the position of the interaction point have been performed.

Figure 2 (left) depicts trajectories of two protons p_1 and p_2 projected onto the (x, y) plane.

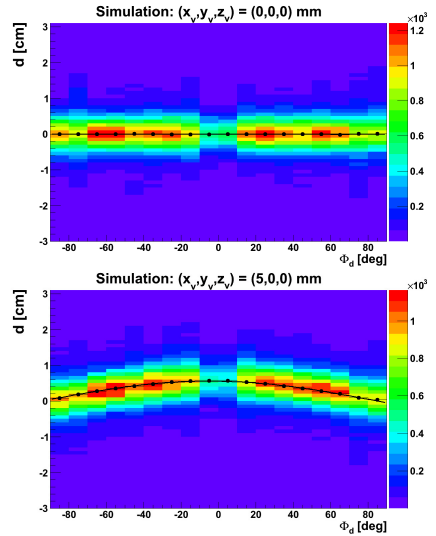
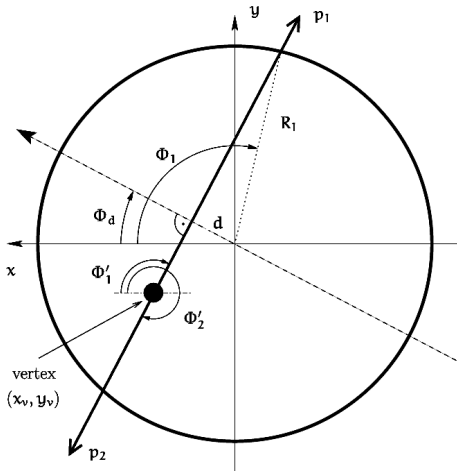


Fig. 2. Left: picture illustrating the concept of the extraction of the x_v and y_v coordinates of the reaction vertex. Adopted from [18]. Right: simulated distributions of $d(\phi_d)$ made for vertex position $(x_v, y_v, z_v) = (0, 0, 0)$ (upper plot) and $(x_v, y_v, z_v) = (5, 0, 0)$ mm (lower plot). Points show positions of the mean of the d -distributions for given ranges of ϕ_d . Line shows a result of the fit of a function given by Eq. (6).

The p_2 proton corresponds to the proton registered in the Mini Drift Chamber. Its reconstructed azimuthal angle, ϕ_2 , is therefore obtained independently of the position of the reaction vertex, always reflecting the ‘true’ value of the emission angle. The p_1 proton is going in the forward direction and it intersects the first plane of the Forward Trigger Hodoscope (FTH) at a radius of

$$R_1 = Z_{\text{FTH}} \tan(\theta_{p_1}), \quad (5)$$

where Z_{FTH} is the distance from the vertex to the Forward Trigger Hodoscope. The reconstruction of the path of the p_1 proton is based on the assumption that the interaction point is located at $(x_v, y_v, z_v) = (0, 0, 0)$. Therefore, reconstructed azimuthal angle, ϕ_1 , differs from the real one, ϕ'_1 . This disagreement causes deviation from the coplanarity corresponding to $\phi'_2 - \phi_1$.

To determine the shift of the reaction vertex, new variables d and ϕ_d are introduced, where d is the distance between the point $(0, 0, 0)$ and the intersection point of dashed line and the solid line in Fig. 2. Dashed line includes point $(0, 0)$ and is perpendicular to the projection of proton’s trajectories. ϕ_d is the azimuthal angle between dashed line and the x -axis.

With the use of the introduced d and ϕ_d variables, the x_v and y_v coordinates of the reaction vertex became two parameters in the following formula

$$d(\phi_d) = x_v \cos(\phi_d) + y_v \sin(\phi_d). \quad (6)$$

Thus, x_v and y_v can be extracted by fit of the above function to the $d(\phi_d)$ distribution as shown in the right-hand side of Fig. 2 for two cases of vertex location, at $(x_v, y_v, z_v) = (0, 0, 0)$ (upper plot) and at $(x_v, y_v, z_v) = (5, 0, 0)$ mm (lower plot).

Figure 3 (left) depicts the angular dependencies between the two protons p_1 and p_2 , used to determine the z_v coordinate of the reaction vertex. In the picture, the reaction vertex is placed on the z -axis at the position of $z_v > 0$.

The trajectory of proton p_2 , reconstructed in the planes of the Mini Drift Chamber, is traced back to the actual reaction vertex, whereas the track of the forward going proton, p_1 , is assumed to origin from the $(0, 0, 0)$ point. Therefore, scattering angle, θ_1 , of the forward going proton deviates from the real value, θ'_1 . The relation between the true and reconstructed values of the scattering angle of the forward going proton can be written as

$$\frac{1}{\tan(\theta'_1)} = \frac{1}{\tan(\theta_1)} \left(1 - \frac{z_v}{Z_{\text{FTH}}} \right). \quad (7)$$

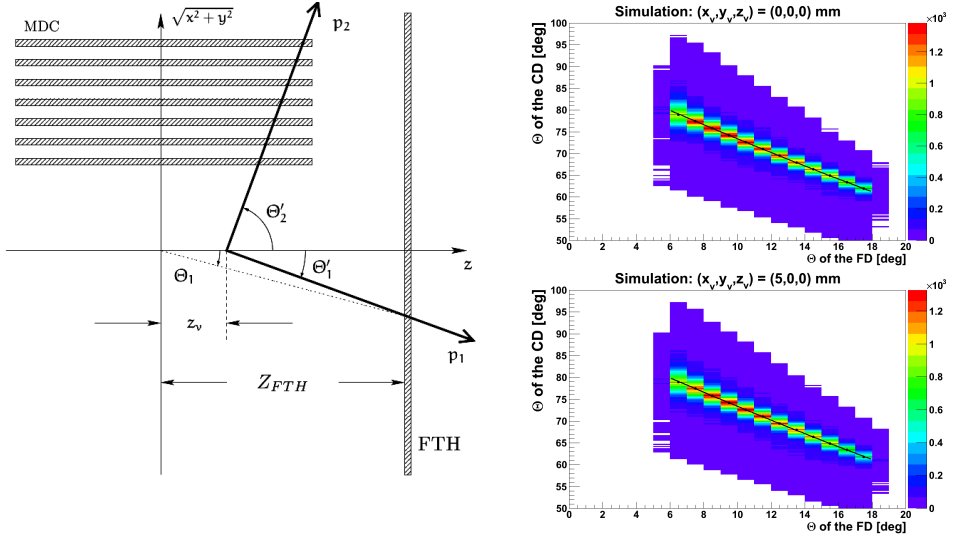


Fig. 3. Left: picture illustrating the concept of the extraction of the z_v coordinate of the reaction vertex. Adopted from [18]. Right: simulated distributions of $\theta'_2(\theta_1)$ made for vertex position $(x_v, y_v, z_v) = (0, 0, 0)$ (upper plot) and $(x_v, y_v, z_v) = (5, 0, 0)$ mm (lower plot). Points show positions of the mean of the θ_{CD} distribution for given ranges of θ_{FD} . Line denotes result of the fit of a function given by Eq. (9) to these points.

Additionally, in an elastic collision the kinematic relation between scattering angles

$$\tan(\theta_1) \tan(\theta_2) = \frac{2m_p}{2m_p + T} \quad (8)$$

must be satisfied, where m_p stands for the proton mass and T is the kinetic energy of the proton beam.

Solving equations (7) and (8) for $\tan(\theta'_2)$ results in

$$\tan(\theta'_2) = \frac{1 - \frac{z_v}{Z_{FTH}}}{\tan(\theta_1) \left(1 + \frac{T}{2m_p}\right)}. \quad (9)$$

Thus, z_v coordinate can be extracted by fitting the $\theta'_2(\theta_1)$ distribution. This is shown in the right-hand side of Fig. 3 for two cases of vertex location, at $(x_v, y_v, z_v) = (0, 0, 0)$ (upper plot) and at $(x_v, y_v, z_v) = (5, 0, 0)$ mm (lower plot).

A set of simulations have been made for different locations of the vertex where only one of the vertex coordinates was changed at once, leaving the others at zero. The accuracy of the method used to extract the vertex position [18] is shown in Fig. 4.

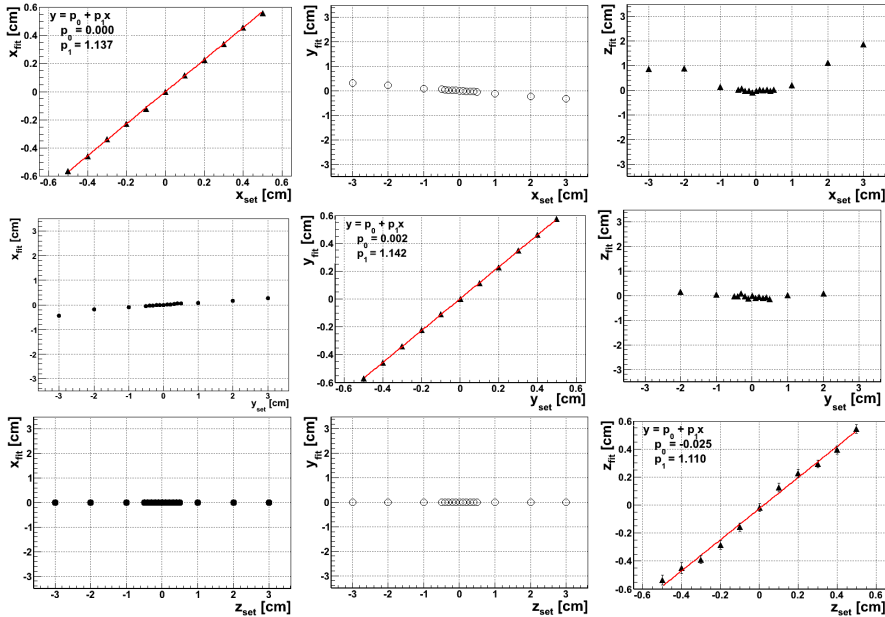


Fig. 4. Plots showing results of Monte Carlo tests made on the x -, y -, z -coordinates of the reaction vertex (first, second and third row, subsequently). See the text for details.

In the first row, pictures corresponding to the change in the x -coordinate (x_{set}) of the vertex are shown. In the second row, the y -coordinate (y_{set}) was changed and in the third row, the z -coordinate (z_{set}). All pictures are distributions of the extracted (fit) value of the given coordinate as a function of the true value (set) of the coordinate being changed. Therefore, points in pictures placed diagonally should be arranged along $\text{fit}(\text{set}) = \text{set}$ line while other distributions should show $\text{fit}(\text{set}) = 0$ behavior.

Fits of the polynomial of the first order to the points in pictures placed diagonally (solid/red lines) show that in all cases, the extracted values deviate slightly from the set ones (up to 14% in the case of the $y_{\text{fit}}(y_{\text{set}})$). This needs to be taken into account while extracting the vertex position in experimental data. We can also notice that if the change in a given coordinate is not bigger than about 0.5 cm, the extraction of other coordinates is accurate.

To determine how the wrong assumption about the vertex position affects the polarization, the polarization was calculated individually for each data sample, simulated with a change in the position of a certain coordinate. Then, each of the simulated data samples was analyzed with the default assumption that the particle going forward origins from the $(x_v, y_v, z_v) = (0, 0, 0)$ point¹.

¹ Tracking algorithm of the Mini Drift Chamber do not assume a certain vertex position.

The result is presented in the left panel of Fig. 5 which shows polarization for different vertex locations.

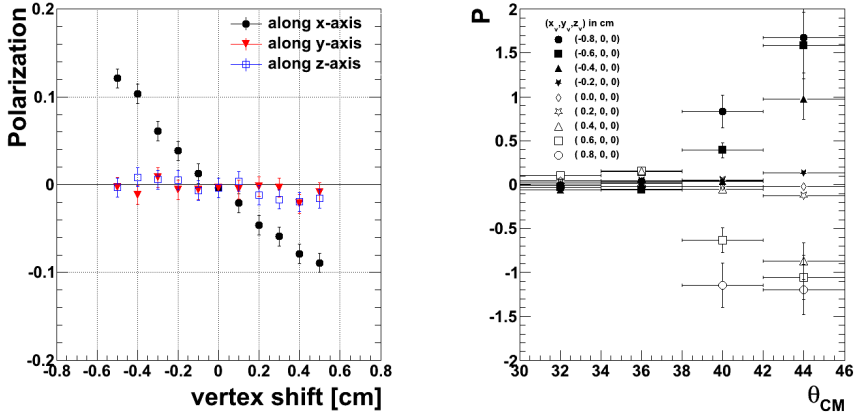


Fig. 5. Left: polarization *versus* vertex shift along the x -, y - and z -axis (see the legend) determined assuming acceptance for the vertex position at $(0, 0, 0)$. Data were simulated at positions as indicated in the figure. Right: polarization as a function of the scattering angle of the forward going proton (center-of-mass scattering), determined from the simulated data with different values of the x -coordinate of the interaction point (see the legend).

While the change of the y_v or z_v coordinate does not have influence on the result, a certain sensitivity of polarization is seen in the case of changing the x_v coordinate of the interaction point. Namely, the calculated value of polarization changes linearly with the shift of the vertex along the x -axis. The influence of moving the interaction point along the x -axis on the polarization depends on the scattering angle of the forward going proton, θ_{CMs} . The right panel of Fig. 5 shows distribution of the polarization as a function of the scattering angle of the forward going proton calculated in the centre-of-mass system, θ_{CMs} , made for different vertex positions (x -coordinate of the vertex was varied). It is seen that for $\theta_{CMs} > 38^\circ$ the polarization strongly deviates from the expected value when changing the x_v coordinate by more than 5 mm. Therefore, since the polarization for higher angles is biased by the systematics, we should restrict the allowed θ_{CMs} angle to less than 38° . On the other hand, the observed dependency, if seen in experimental data, would be a clear sign of the wrong assumption of the x -position of the interaction point. It is important to notice that, based on the results shown in Fig. 6 (left) in order to achieve uncertainties of the polarisation determination of about 0.03, the vertex position must be controlled with the accuracy better than 1 mm.

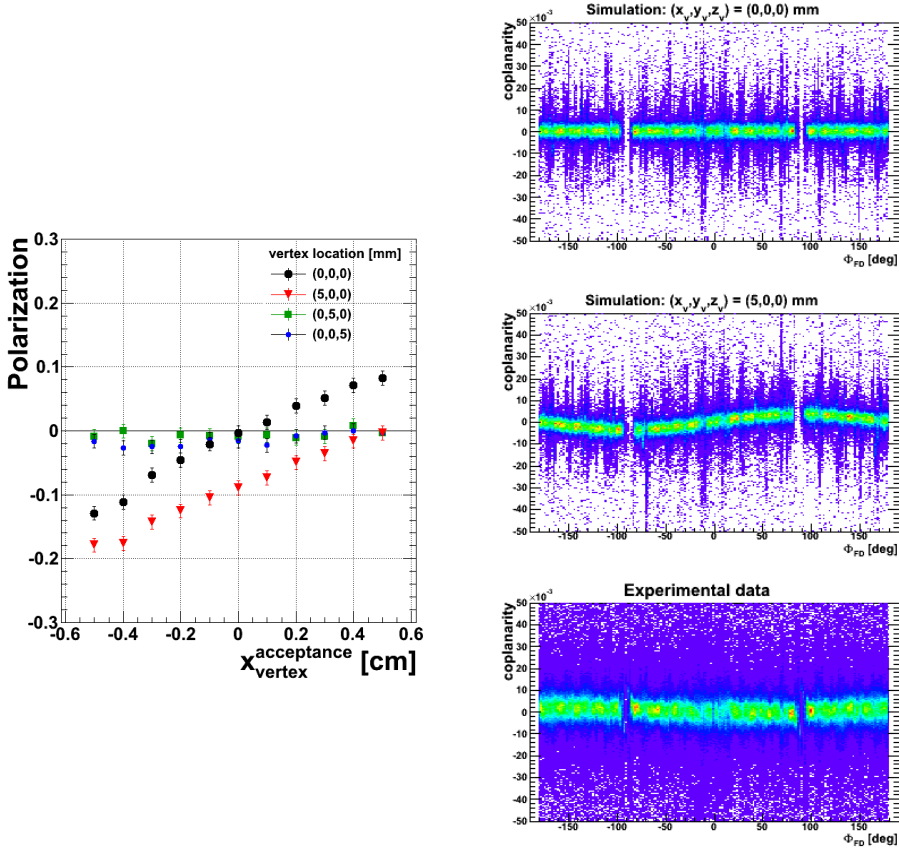


Fig. 6. Left panel: polarization *versus* shift of the vertex location along the x -axis, taken in determining the acceptance correction, $x_{\text{vertex}}^{\text{acceptance}}$. The polarization was calculated for four locations of the interaction point (see the legend). Right side: coplanarity dependence on the protons' azimuthal angle.

In the left panel of Fig. 6, a result of further studies is shown how, wrongly assumed, location of the interaction point influences the polarization. Data, simulated with four different vertex positions (as indicated in the legend), have been acceptance corrected assuming different values of the x_v coordinate, $x_{\text{vertex}}^{\text{acceptance}}$. In this case, a result is similar as shown in Fig. 5. It shows that in order to control polarisation determination with the precision of about 0.03, we need to control the determination of the x -coordinate of the vertex with the precision of about 1 mm. Comparison of circles (black) and triangles (red) indicates that this conclusion is independent of the 'true' position of the vertex, at least within the range of 5 mm. It might be noticed as well that data, generated with y_v or z_v set to 5 mm and corrected to different $x_{\text{vertex}}^{\text{acceptance}}$, do not influence the polarization significantly.

Another way to control the location of the vertex position in the experiment is to monitor the coplanarity, C , defined as

$$C = \frac{(\vec{p}_1 \times \vec{p}_2) \cdot \vec{p}_{\text{beam}}}{|\vec{p}_1 \times \vec{p}_2| \cdot |\vec{p}_{\text{beam}}|}, \quad (10)$$

where \vec{p}_1 and \vec{p}_2 correspond to two scattered protons and \vec{p}_{beam} is the vector of the beam. Coplanarity dependence on the protons' azimuthal angle shows sinusoidal behavior for misallocated vertex. This is shown in the right-hand side of Fig. 6. The left plot corresponds to simulated data with the vertex located at $(x_v, y_v, z_v) = (0, 0, 0)$ cm, the $C(\phi)$ distribution is flat. Moving the vertex position to point $(x_v, y_v, z_v) = (0.5, 0, 0)$ cm results in a sinusoidal shape. This is shown in the middle plot in the right-hand side of Fig. 6. Experimental data are presented in the lower, right corner of Fig. 6.

2.2. Tilt of the beam

The maximum allowed range of tilts of the beam at the WASA-at-COSY is between -0.05 mrad and 0.05 mrad (symmetrically around the z -axis) [19]. To determine how the tilt of the beam affects the polarization, the beam was leaned in the yz -plane or xz -plane at different α_x and α_y angles respectively. In Fig. 7, the polarization as a function of the α angle for both types of studied beam tilts is shown. There are no effects observed in the studied range of the α angle ($\alpha \in [-0.5, 0.5]$ mrad) except that polarization slightly differs from zero (up to 0.01).

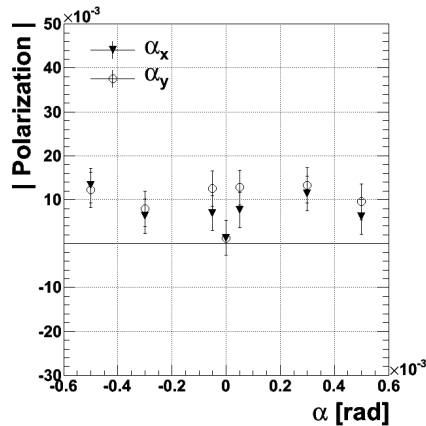


Fig. 7. Distribution of the polarization as a function of the degree of the beam tilt in the yz -plane (filled triangles) and xz -plane (open circles). (Simulations.) The studied range is by factor of ten larger than the range of the possible tilt allowed by the COSY optics [19].

3. Summary

Methods to monitor the location of the vertex have been demonstrated and it was shown how the misallocation of the vertex impacts the obtained degree of polarization. The study concluded that to have systematic uncertainty of the polarization smaller than 0.03, we need to control the position of the interaction point with the precision higher than 1 mm. In this article, we presented three methods for the determination of the vertex position: (i) based on the $d(\phi)$ distribution, (ii) coplanarity distribution, (iii) polarization as a function of θ_{CMs} . Due to the large statistics of collected data and the usage of the listed methods, the vertex position will be determined with the precision much better than 1 mm. Due to the large sensitivity of the result to the scattering angle, it is better to calculate polarization taking into account the scattering angle not bigger than $\theta_{\text{CMs}} = 38^\circ$.

It was also presented that the beam, tilted within the maximum allowed range, should have no significant influence on the obtained degree of polarization.

We acknowledge support by the Polish National Science Center through grant No. 2011/03/B/ST2/01847, by the FFE grants of the Research Center Jülich, by the EU Integrated Infrastructure Initiative Hadron Physics Project under contract number RII3-CT-2004-506078 and by the European Commission under the 7th Framework Programme through the Research Infrastructures action of the Capacities Programme, Call: FP7- INFRASTRUCTURES-2008-1, Grant Agreement N. 227431.

REFERENCES

- [1] M. Abdel-Bary *et al.*, *Eur. Phys. J.* **A16**, 127 (2003).
- [2] P. Moskal *et al.*, *Phys. Rev.* **C69**, 025203 (2004).
- [3] H. Petren *et al.*, *Phys. Rev.* **C82**, 055206 (2010).
- [4] P. Moskal *et al.*, *Eur. Phys. J.* **A43**, 131 (2010).
- [5] H. Calen *et al.*, *Phys. Lett.* **B366**, 39 (1996).
- [6] H. Calen *et al.*, *Phys. Rev. Lett.* **79**, 2642 (1997).
- [7] F. Hibou *et al.*, *Phys. Lett.* **B438**, 41 (1998).
- [8] J. Smyrski *et al.*, *Phys. Lett.* **B474**, 182 (2000).
- [9] A.M. Bergdolt *et al.*, *Phys. Rev.* **D48**, 2969 (1993).
- [10] P. Moskal *et al.*, *Phys. Rev.* **C79**, 015208 (2009).
- [11] P. Moskal, [arXiv:hep-ph/0408162](https://arxiv.org/abs/hep-ph/0408162).
- [12] S. Abd El-Samad *et al.*, *Phys. Lett.* **B522**, 16 (2001).

- [13] R. Czyżykiewicz *et al.*, *Phys. Rev. Lett.* **98**, 122003 (2007).
- [14] P. Winter *et al.*, *Eur. Phys. J.* **A18**, 355 (2003).
- [15] F. Balestra *et al.*, *Phys. Rev.* **C69**, 064003 (2004).
- [16] P. Moskal, M. Hodana, *J. Phys. Conf. Ser.* **295**, 012080 (2011).
- [17] M. Altmeier *et al.*, *Phys. Rev. Lett.* **85**, 1819 (2000).
- [18] L. Demirors, Ph.D. Thesis, Hamburg University, 2005.
- [19] D. Prashun, private communication, 2013.